THIRTEENTH EUROPEAN ROTORCRAFT FORUM

Paper No. 63 210

September 8-11, 1987
ARLES, FRANCE

AN EXPERIMENTAL STUDY OF THE AERODYNAMIC CHARACTERISTICS OF THREE MODEL HELICOPTER FUSELAGES

S.R. Ahmed, J. Amtsberg
DFVLR, GERMANY

ASSOCIATION AERONAUTIQUE ET ASTRONAUTIQUE DE FRANCE

AN EXPERIMENTAL STUDY OF THE AERODYNAMIC CHARACTERISTICS OF THREE MODEL HELICOPTER FUSELAGES

S.R. AHMED, J. AMTSBERG
Deutsche Forschungs- und Versuchsanstalt
für Luft- und Raumfahrt e.V. (DFVLR)
Braunschweig, W.-Germany

Abstract

The aerodynamic characteristics of three fuselage configurations, typical for the current generation of helicopters, are evaluated on the basis of a wind tunnel study.

A 1:7-scale model fuselage with variable rear end was used to generate a streamline, upswept rear-end and flat back rear-end helicopter fuselage. Wind tunnel tests were conducted at 60 m/s. Rotor flow was not simulated.

The analysis is based on six-component force measurements, surface pressure measurements and flow field survey in the wake. Emphasis is placed on the flight cruise condition of incidence $\alpha = -5°$ and zero yaw.

1. Introduction

The increasing attention being paid by the manufacturers to the aerodynamics of helicopter fuselages is prompted by the need to reduce drag and vibration, increase flight speed and fuel efficiency, and improve the flying qualities of modern helicopters. In the past helicopters were designed mainly to hover so that rotor aerodynamics was the main concern. With forward speeds approaching 300 km/h and above, fuselage aerodynamics start playing a decisive role in defining the performance of a helicopter.

Although flight tests are crucial to helicopter development, due to the costs involved they are seldom used for basic research in fuselage aerodynamics. Wind tunnel tests play here the fundamental role for project studies and basic research. Besides low costs, ease of test procedures etc., many dangerous flight conditions, otherwise impossible to be investigated, can be simulated in the wind tunnel. Since the fuselage flow for conventional helicopter designs is practically incompressible, Mach-number similarity between model and full-scale need not be rigorously imposed. However, if large differences exist in the flight test and wind tunnel Reynolds-number, discrepancies especially in drag behaviour occur.

The fuselage of a helicopter underlies operational requirements which impose unfavourable geometric constraints on the afterbody geometry. The bluff aft-fuselage shape creates an extensive region of separation in the rear, resulting in a large pressure drag. An upswept rear end, unfavourably de-

signed, leads to strong longitudinal vortices emanating at the side/rear end slant edge which may adversely effect drag, flight stability and fin effectiveness, [1], [2]. Streamlined fuselage configurations in which there is a gradual transition from main body to tail boom exhibit for negative incidences unstable behaviour caused by alternate vortex shedding off the aft portion. A critical parameter for fuselage drag and stability is thus the aft body shape. All three fuselage configurations mentioned above are represented in the current generation of helicopters and thus their aerodynamic performance is of interest.

2. Experimental Set-up and Test Procedure

The model investigated was a 1:7 scale helicopter fuselage with interchangeable rear ends, Fig. 1. Front and middle part of the model remained common to all configurations. Through change of the rear part a streamline, upswept and flat back model version could be realized. The upswept rear-end model has been the subject of earlier studies [1], [2] where besides wake surveys also pressure and force measurements were conducted.

Wind tunnel tests were performed in the open test section of the DFVLR low speed wind tunnel in Göttingen. This facility, described in [3], is an open test section closed return wind tunnel with 3 m x 3 m cross section and a test section length of 5.86 m. The streamline and flat back models were mounted in the tunnel via a sting through the tail boom Fig. 2a. On the other hand, the swept back rear end model was mounted upside down on a vertical mast as shown in Fig. 2b. A strain gauge balance, arranged inside the model was used to measure the aerodynamic forces.

One half of the model (including the rear end) was instrumented with pressure taps distributed over the periphery of various sections indicated in Fig. 1. The streamline model has a total of 190, the upswept rear end model 218 and the flat back model 143 pressure taps. Scanivalves for pressure data acquisition were installed within the model.

Flow field survey was done with a ten hole directional probe, Fig 3, ([4], [5]) which has four orifices on the conical tip arranged such as to make the pressure difference between one opposing pair sensitive primarily to incidence and the other to flow yaw. Incidence rotations are imposed until the pressure in the opposing pair of orifices is equalized; in this condition the probe tip points nominally in the direction of local incidence. Calibration curves are used to compute the local yaw angle from the pressure difference shown by the other pair of orifices. The pressure in the central tip orifice and mean of pressures in four orifices on the cylindrical sleeve is a function of local total and static pressures respectively. Thus magnitude and direction of the local velocity vector and local pressure could be determined. The orifice on the rear-end of the probe serves to indicate flow re-

versal. The probe was mounted on a carriage providing remote controlled rectangular cartesian translation in the test section.

Wind tunnel tests were conducted at a wind speed of 60 m/s. The ratio of model front to tunnel nozzle area was about 1 %. The moment reference point for the three configurations is shown in Fig. 1, whereby these coordinates are same for the streamline and flat back versions.

Force measurements were done in the angle of incidence range of $\alpha = \pm 30°$ in increments of 1°, 2° and 5°; angle of yaw was varied between $\beta = 5°$ to $-20°$ in 5° steps. Surface pressure measurements covered an angle of incidence range of $\alpha = -9°$ to 20° and yaw angle values $\beta = \pm 20°$. Flow field surveys (in planes perpendicular to free stream) for some of these incidence and yaw angle values were obtained for the streamline and flat back models at stations 980. mm and 1305. mm downstream from model nose. For the upswept rear end configuration such stations were located at 1070. mm, 1645. mm and 2130. mm downstream of the model nose. Tailboom mounting of the other two models prevented the location of field survey planes at the last two locations.

A computerized data acqisition and reduction system enabled rapid flow field surveys. The continuously recorded probe data was integrated over 0.2 s to arrive at the average values finally recorded. Force and pressure measurement data was processed in a similar manner whereby surface pressure values were averaged over 2 s and force values over 0.6 s. Choice of these integration times is based on a calibration analysis of the system.

3. Discussion of experimental results

In what follows only a representative set of results are presented from the large amount of data generated during the tests. Main and tail rotor flow was not simulated. An analysis of the aerodynamic qualities of the three fuselage shapes is attempted on the basis of six-component force measurements, pressure distribution and flow field survey in the wake.

3.1 Force measurements

The effect of incidence on the drag behaviour of the three fuselage configurations is seen in Fig. 4a. Highest values of drag in the range of incidence $\alpha = 2°$ to $-25°$ are obtained for the upswept rear-end configuration. The upswept rear-end model contains in its flow two physical phenomena in the aft region which generate significant pressure drag. The wake region may, depending upon the angle of incidence, contain a 'dead water' type of 'separation bubble' or a smaller separation bubble with two longitudinal vortices at its edge with their axis following the upswept edges and tail boom. The

vortices emanate at the slanted side face/upswept rear-end edge [1], [2].

The kinetic energy content of the vortices, or in other words the low pressure peaks created as a consequence on the upswept rear end generate the higher values of drag, especially in the negative incidence range as seen in Fig. 4 (see also [6]). For still lower values of incidence the side/bottom face edges become progressively more slanted to the free stream so that these too generate vortices. Since the projected frontal area also increases causing an increase in the net drag force, the effects cumulate to exhibit the drag rise demonstrated. Positive incidence angles have the effect of lowering the slant angle of the upswept rear end, so that the longitudinal vortices dissipate. The breakdown of this vortex structure apparently lowers the drag value. This phenomenon has been observed in the case of fastback automobiles [5], where the base slant angle was varied.

With increasing positive incidence, the role of vortex generation is taken up gradually by the edges of side/top face. However as these are well rounded, a significant effect is conjectured to be present at angles of incidence larger than those measured in Fig. 4a. The stagnation of C_D values in the range of α = 5° to 20° indicates the influence of these compensating effects and absence of a well defined wake structure.

The almost symmetric variation of the drag curve for the flat back fuselage configuration is primarily the result of the sharply defined separation line of the flow. The wake emanates, for the incidence range investigated, at the periphery of the base and a significant change in the wake cross section with incidence is not present. Since the drag coefficient value shown in Fig. 4a is based on the model cross section, and the net drag value increases with incidence due to increase of projected frontal area, the drag rise noticed is apparently caused by the increased frontal area exposed to the onset flow.

Inhibition of pressure drag through a smooth transition from the main body to the tail boom, as effected in the 'streamline' model shows the payoff achieved in Fig. 4a. For the cruise condition of α = -5°, this configuration has a drag value amounting to 1/4 to 1/3 of that for the upswept rear-end or flat back models respectively. Over the incidence angle range of α = -5° to +10° this favourable low value of drag is practically maintained.

All three fuselage models experience a negative lift force in the negative incidence range; for the upswept rear end model this range extends upto about 7° as seen in Fig. 4b. This is mainly caused by the pressure distribution generated in front region of the fuselage (as to be seen later in Fig. 8).

The almost same gradient of the C_L-α curves of all configura-

tions in the negative incidence range indicates that the lift behaviour is governed by the pressure distribution generated on the front part of the fuselage. The streamline model exhibits here also the favourable low negative lift values in the range of $\alpha = -5°$ to 10°. High values of negative lift seen in Fig. 4b for the upswept rear-end model are due to the low pressures created on the upswept rear-end surface.

Streamline bodies with little or no separation in their flow field are more susceptible to changes in direction of onset flow. This is borne out by the pitching moment curves plotted in Fig. 4c. With little or no separation on the body surface, as is tne case for the streamline model fuselage, the pressure at each surface point is mutually dependent without the damping effect of a region of separation which, for example, is present in the form of a wake in the flow field of the other two models studied. Due to this the streamline fuselage curve exhibits a relatively steep gradient for the pitching moment.

Effect of yaw on the Lift, Drag and Pitching moment characteristics of the fuselages are shown in Fig 5. Interesting to note is the simularity in drag behaviour with yaw for the streamline and the flat back models (Fig. 5a). Whereas in the case of the streamline model the afore mentioned intense depending of surface pressure on onset flow variation appears to be the cause of the drag sensitivity to yaw, the drag change for the flat back model can be explained to be effected by base pressure changes in the strongly coupled attached flow and wake flow of this short fuselage. Lift and Pitching moment values remain almost stagnant, Fig. 5b and c, over the yaw angle range investigated.

Characteristic results for the side force, rolling moment and yawing moment variation with the angle of yaw in the range of $\beta = -5°$ to 20° are shown in Figs. 6a, b and c. While the streamline and upswept rear end models show similar side force variation behaviour over β values between -5° to 10°, the flat back version exhibits a linear variation with a steeper gradient over the whole range of yaw angles investigated, Fig. 6a. Difference in rolling moment behaviour with yaw is demonstrated by the streamline configuration in Fig. 6b, whereby its low values stand in contrast to the almost same type of change for the other two configurations (for values of β between 0° and 12°). Significant difference in yawing moment curves of the three configurations, as seen in Fig. 6c, can not be observed.

3.2 Pressure distribution on fuselage surface

An isometric view of the pressure distribution in various cross sections of the fuselage configurations studied is depicted in Fig. 7. From low drag point of view, it is desirable to achieve a pressure distribution as uniform as possible over the cross section contour. In the front part of the fuselage, a deviation from this condition is tolerable as

flow is accelerating and boundary layer is comparatively thin. In the rear portion of the fuselage this condition is however important to attain a low drag value.

A look at Fig. 7a bears out this explanation for the low drag behaviour of the streamline fuselage configuration. In contrast, the aft portion of the upswept fuselage configuration (Fig. 7b) exhibits pressure peaks at the slant edge caused by the longitudinal vortices generated. These pressure peaks are noticeable also along the tail boom.

Another interesting feature of the pressure results is the similarity of the pressure distribution in front portion of all three fuselage configurations. This observation is deceptive, since the differences, even though small, create through the integral effect over the body surface the differences in the aerodynamic behaviour. Fig. 7 also indicates validity of these observations for the yaw angle $\beta = -15°$. In Fig. 8 the pressure distribution along the top and bottom centre line of the three fuselage configurations is shown. As noted above, the pressure values on the front part of the fuselages, are almost identical and start deviating in the rear. Negative values of Lift, as noted earlier in Fig. 4, are primarily caused by the contribution of the front fuselage portion.

3.3 Flow field survey in wake

To gain an insight into the structure of the flow field, especially in the wake region, the cross flow velocity distribution ($V_{y,z}$ vector plots) was determined in selected planes perpendicular to the onset flow. Experimental constraints prevented the identical location of these planes for all three fuselage configurations studied.

Fig. 9 shows the flow field survey results in an isometric view for the cruise condition, $\alpha = -5°$ and $\beta = 0°$. As expected from previous observations, the strongest cross flow is seen in the flow field of the upswept rear end fuselage (Fig. 9b), which clearly indicates a pair of strong upwash creating and counter rotating votices, with their axis aligned along the tail boom. This vortex structure is present at the tail rotor location and persists further downstream, (see [2]). Filling up of the wake proceeds, as seen in Fig. 9a and c, for the streamline and flat back fuselage versions, through inflow mainly from the sides and below. This does not lead to the characteristic strong vortex formation as mentioned above.

In Fig. 10 the effect of yaw on the cross flow in wake is investigated. View seen is downstream, in planes perpendicular to onset flow. Surprisingly, all three fuselage configurations show similar cross flow structures in the yawed condition ($\beta = -15°$). Under yaw, the front fuselage portion appears to generate a similar cross flow in the wake as observed earlier for the upswept rear-end fuselage. A conclu-

sive result as to whether this leads to formation of vortices also for the streamline and flat back fuselages which persist further downstream is not to be inferred from data available.

4. Conclusions

1. A major portion of aerodynamic drag of conventional helicopter fuselages stems from pressure drag.

2. The pressure drag is essentially created by either a 'dead water' type of separation and/or strong longitudinal vortices in the wake.

3. A drastic reduction of the drag by an amount two thirds to three fourths of the value for other fuselage configurations was obtained by a gradual transition of the cross section of the main body to the tail boom.

4. The streamlining through gradual transition of the cross section from main body to the tail boom resulted in an overall improvement with regard to Lift, Pitching-, Rolling- and Yawing moments.

Acknowledgement

The results reported here represent a part of the work done under GARTEUR Action Group AG04 activities by the authors.

References

[1] J. Amtsberg, S.R. Ahmed, Wake characteristics and aerodynamic forces of a helicopter model fuselage, Forum Proceedings of the 9th European Rotorcraft Forum, Paper No. 4, Sept. 1983.

[2] J. Amtsberg, S.R. Ahmed, Influence of rear end spoiler on aerodynamic characteristics and wake structure of a helicopter fuselage, Forum Proceedings of the 11th European Rotorcraft Forum, Paper No. 33, Sept. 1985.

[3] F.W. Riegels, W. Wuest, Der 3-m-Windkanal der Aerodynamischen Versuchsanstalt Göttingen, Zeitschrift für Flugwissenschaften, Nr. 9, pp. 222-228, 1961.

[4] S.R. Ahmed, W. Baumert, The structure of wake flow behind road vehicles, Symposium on Aerodynamics of Transportation, (Editors T. Morel et al), ASME New York, pp. 93-103, 1979.

[5] S.R. Ahmed, Wake structure of typical automobile shapes, Journal of Fluids Engineering, Vol. 103, pp. 162-169, 1981.

[6] J. Seddon, Aerodynamics of the helicopter fuselage upsweep, Forum Proceedings of the 8th European Rotorcraft Forum, Paper No. 2.12, Sept. 1982.

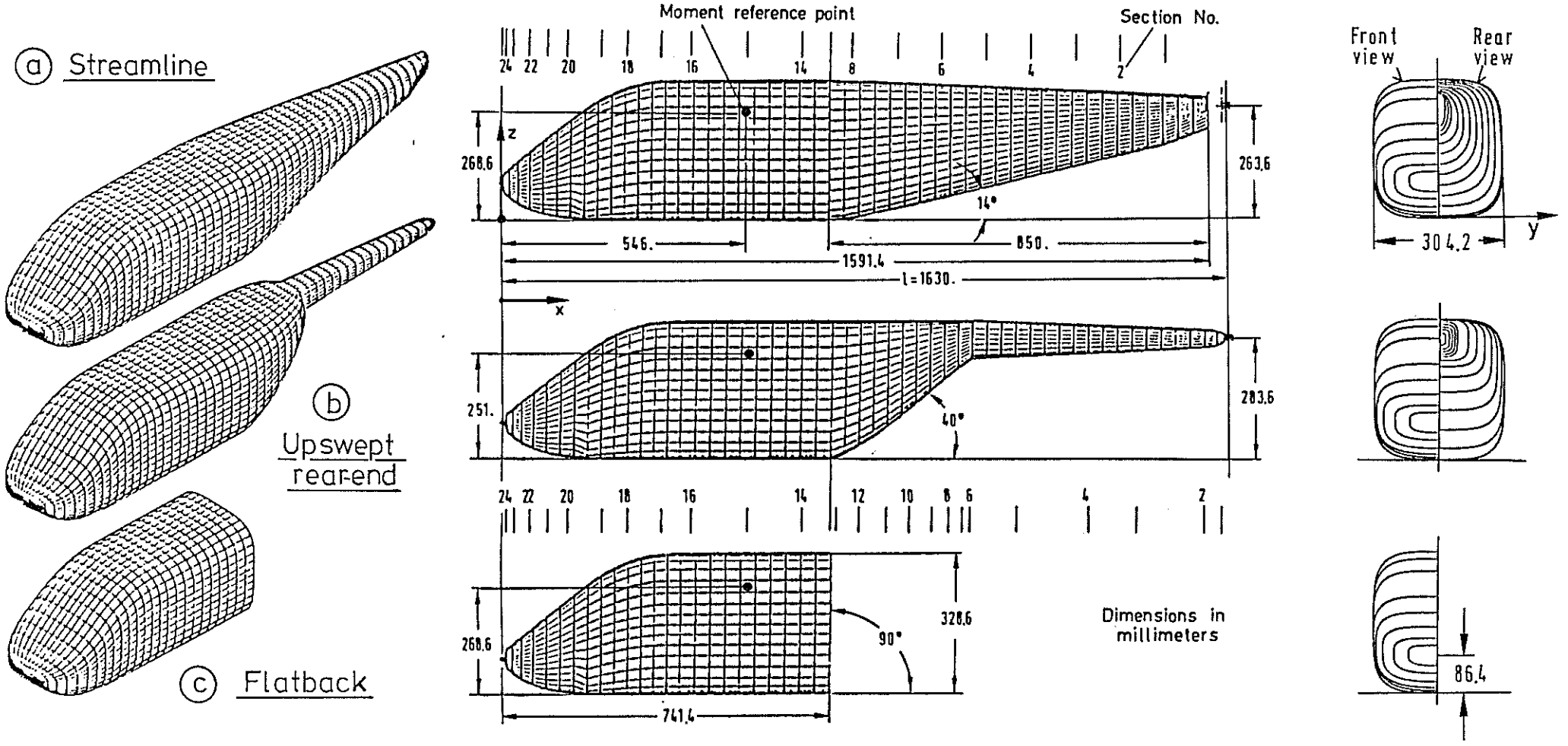

Fig. 1: Fuselage models. Pressure taps are distributed on cross section contour at stations indicated.

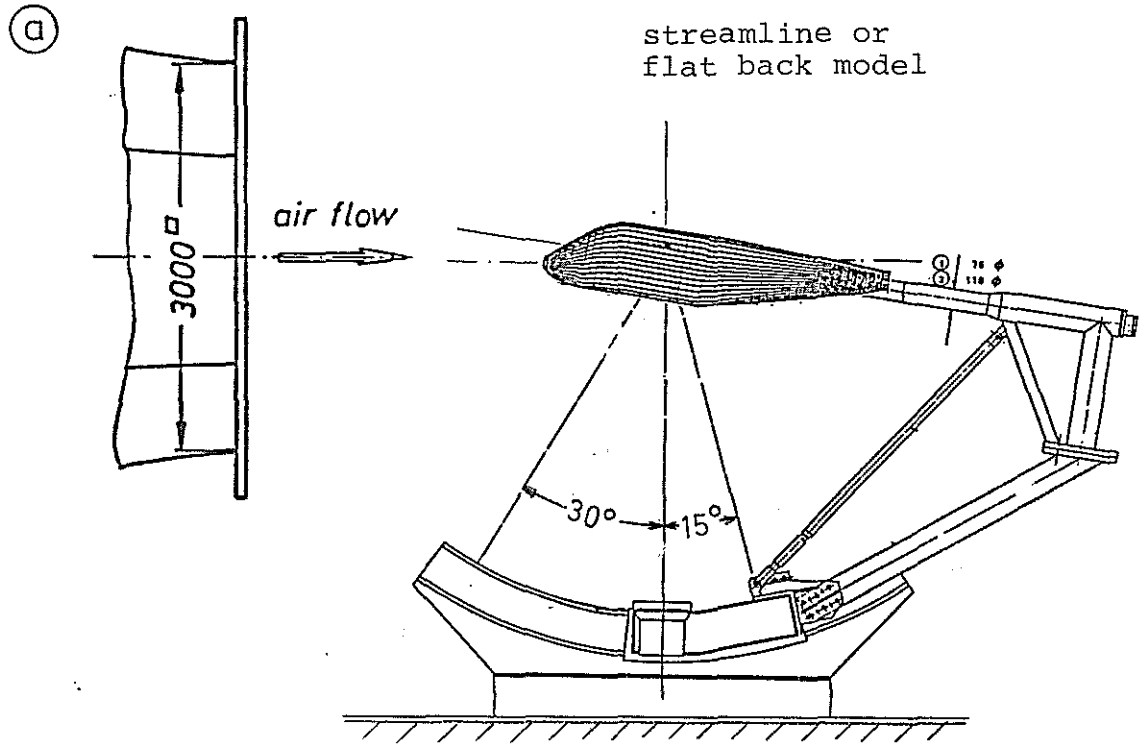

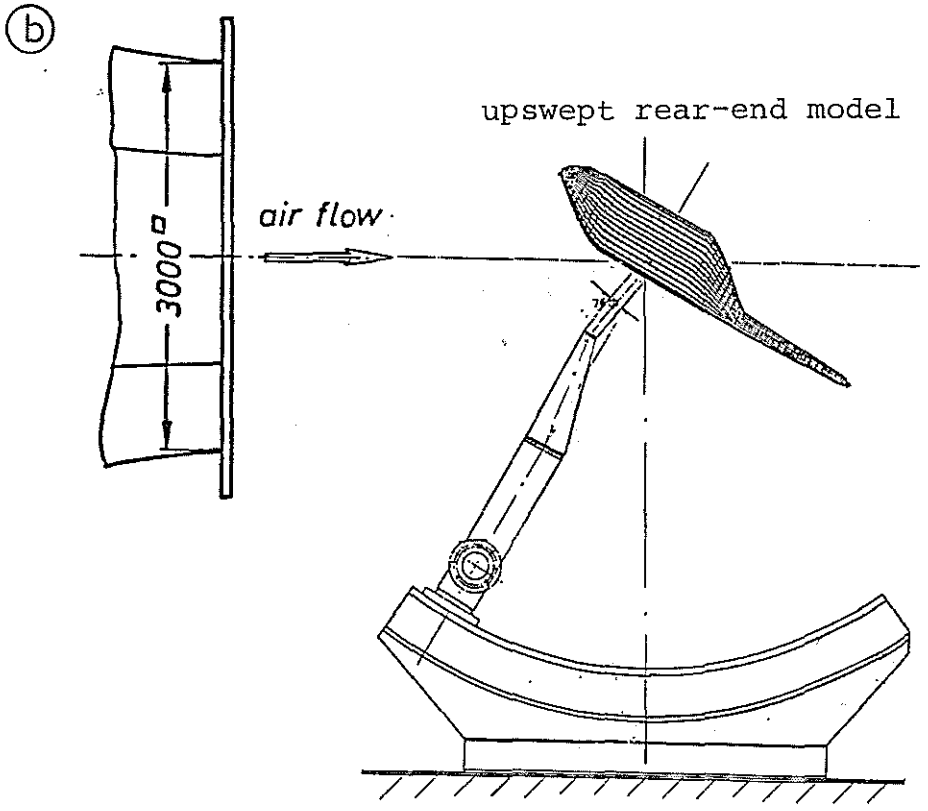

Fig. 2: Test set-up in wind tunnel

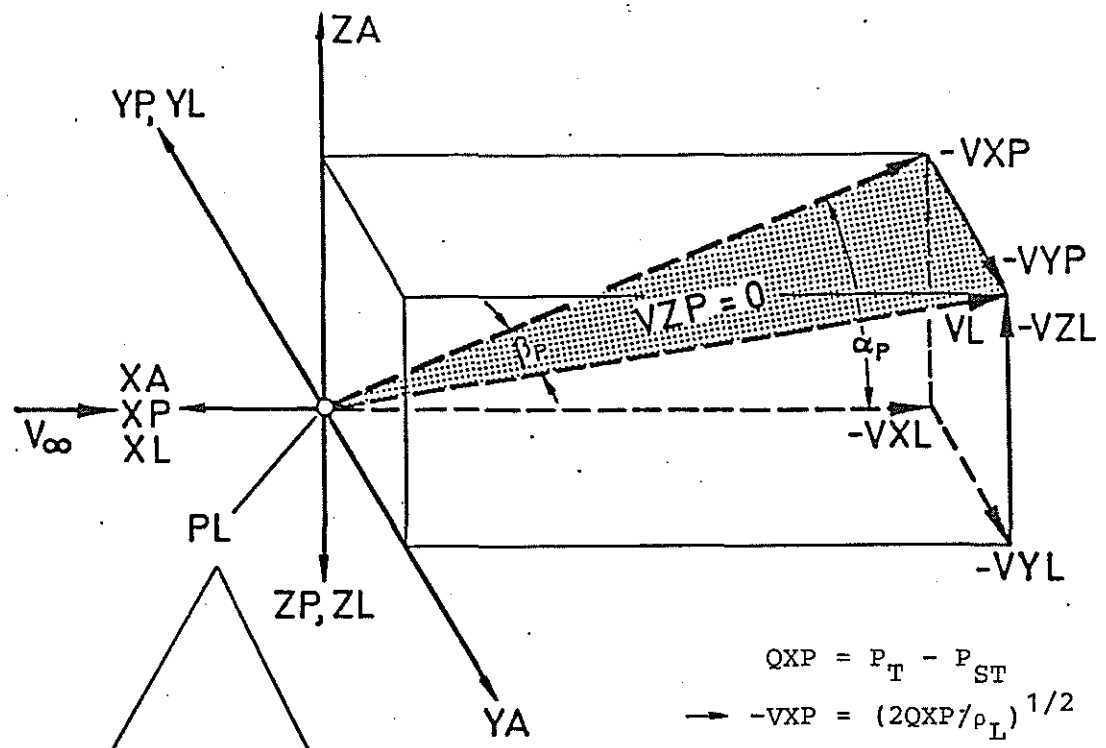

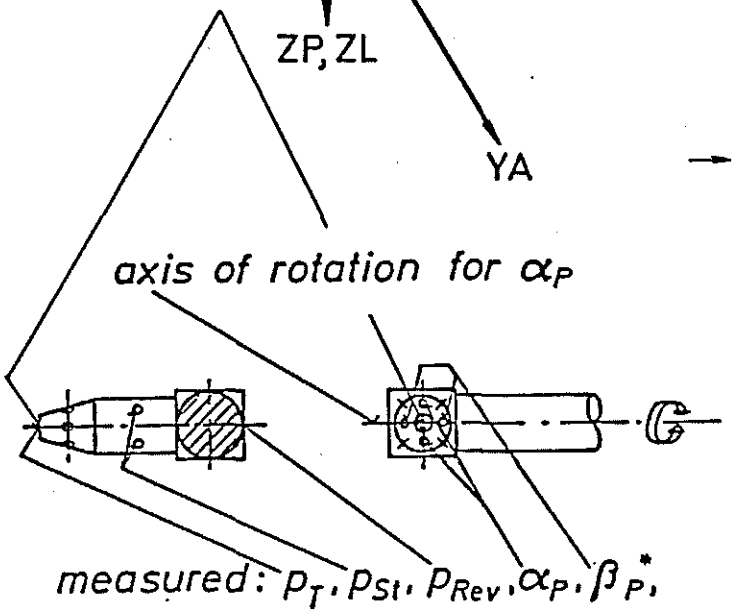

$$QXP = P_T - P_{ST}$$

$$\rightarrow -VXP = (2QXP/\rho_L)^{1/2}$$

$$\rho_L = \frac{P_{ST} + BA}{R \cdot TEMP}$$

$$VL = \frac{-VXP}{\cos\beta_p}, \quad VL = \frac{VL}{V_\infty}$$

or $-VXP = VL \cdot \cos\beta_p$

$-VYP = VL \cdot \sin\beta_p$

$-VXL = -VXP \cdot \cos\alpha_p$

$-VYL = -VYP$

$-VZL = -VXP \cdot \sin\alpha_p$

Index	*L*	*local*
	p	*probe*
	T	*total*
	St	*static*
	Rev	*revers*

$$-VXL = VL \cdot \cos\beta_p \cdot \cos\alpha_p$$
$$-VYL = VL \cdot \sin\beta_p$$
$$-VZL = VL \cdot \cos\beta_p \cdot \sin\alpha_p$$

* β_p *from calibration curve*

BA Barometric Pressure [Nm^{-2}]

R = 287.1 [Nm kg^{-1} $Grad^{-1}$]

TEMP Temperature [K]

Model position upside down: drawn

Model position upside up : YA = -YA
ZA = -ZA

Fig. 3: Flow field survey probe and velocity component evaluation procedure

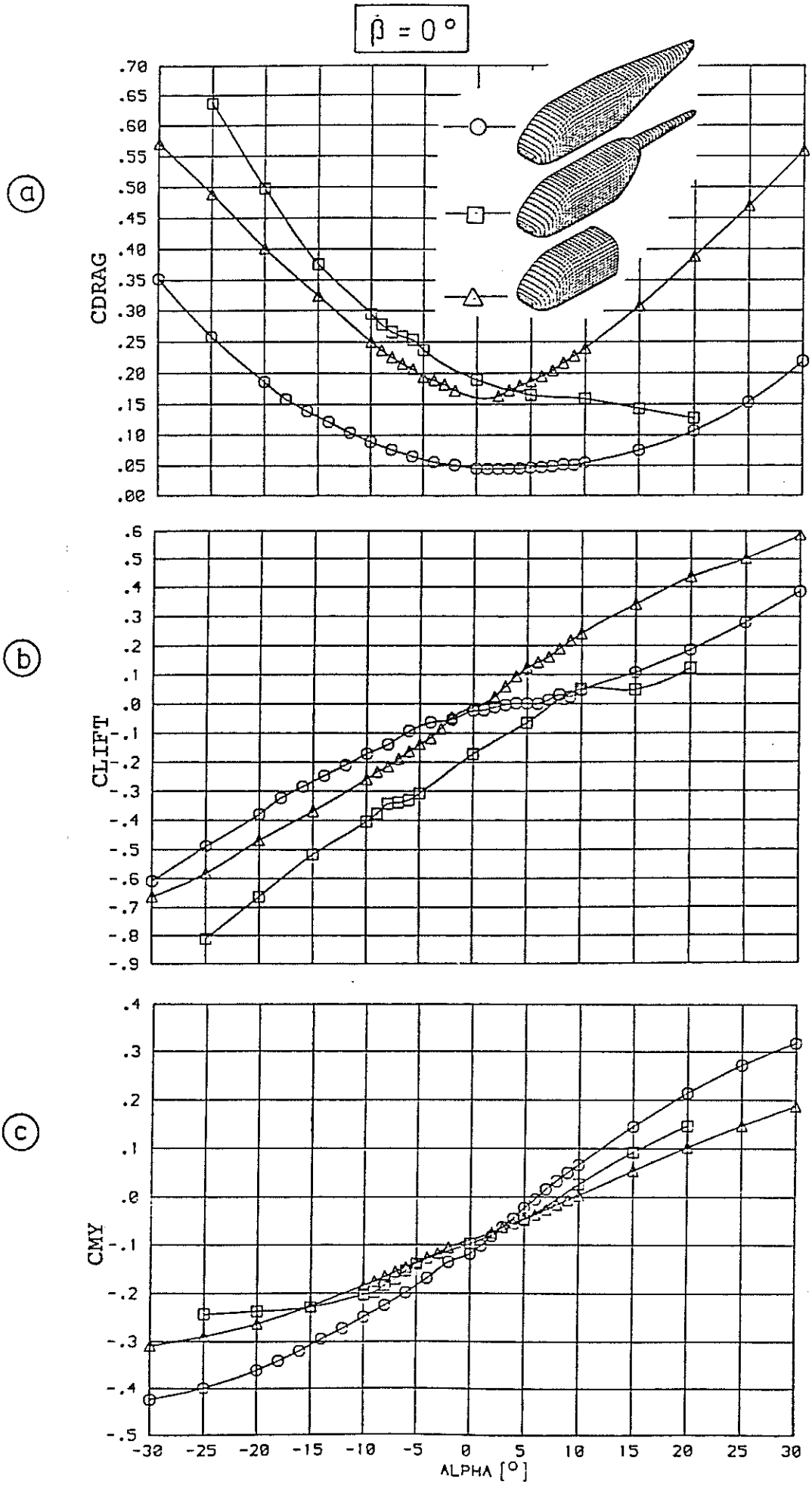

Fig. 4: Variation of Drag-, Lift- and Pitching moment coefficients with angle of incidence

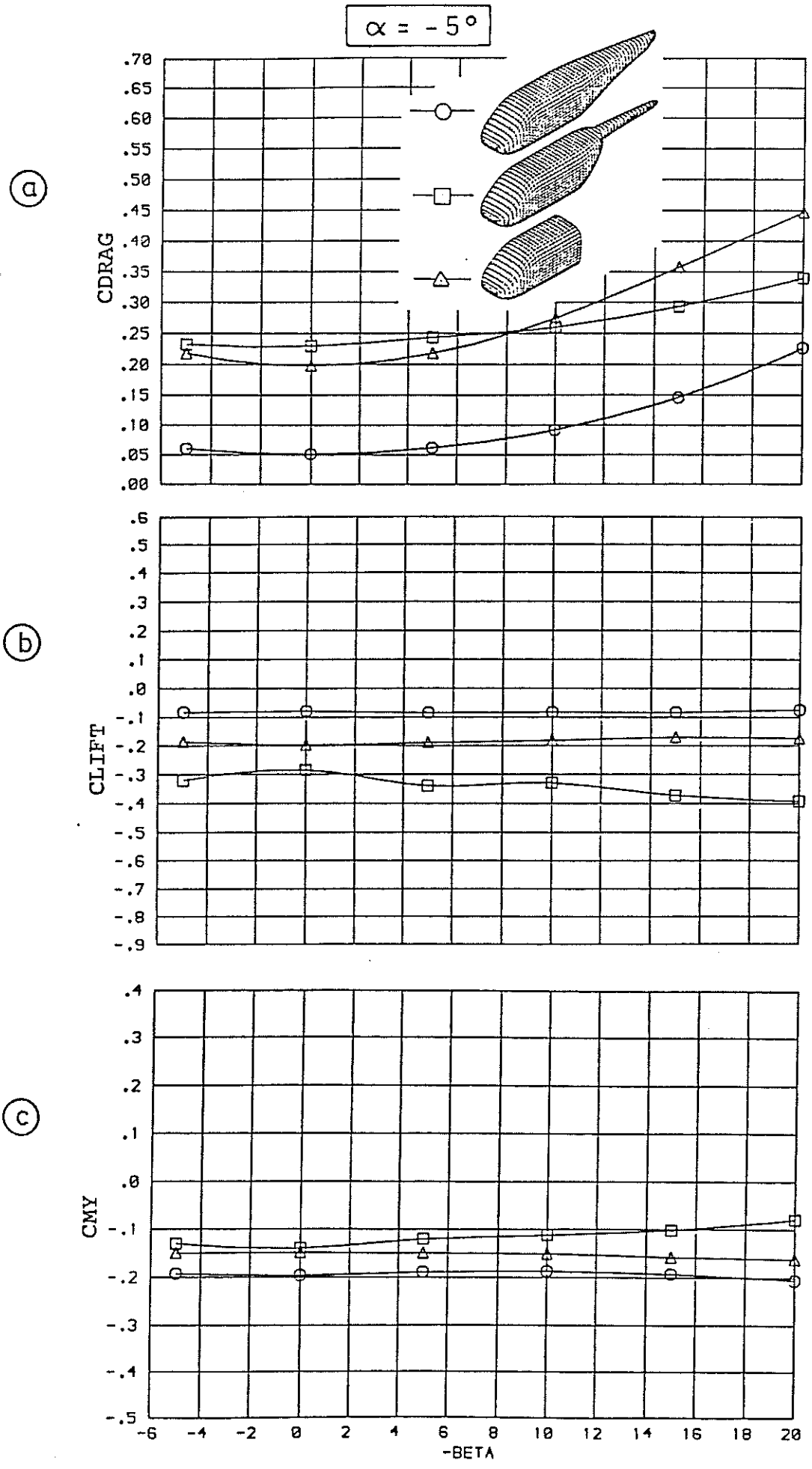

Fig. 5: Variation of Drag-, Lift- and Pitching moment coefficients with angle of yaw

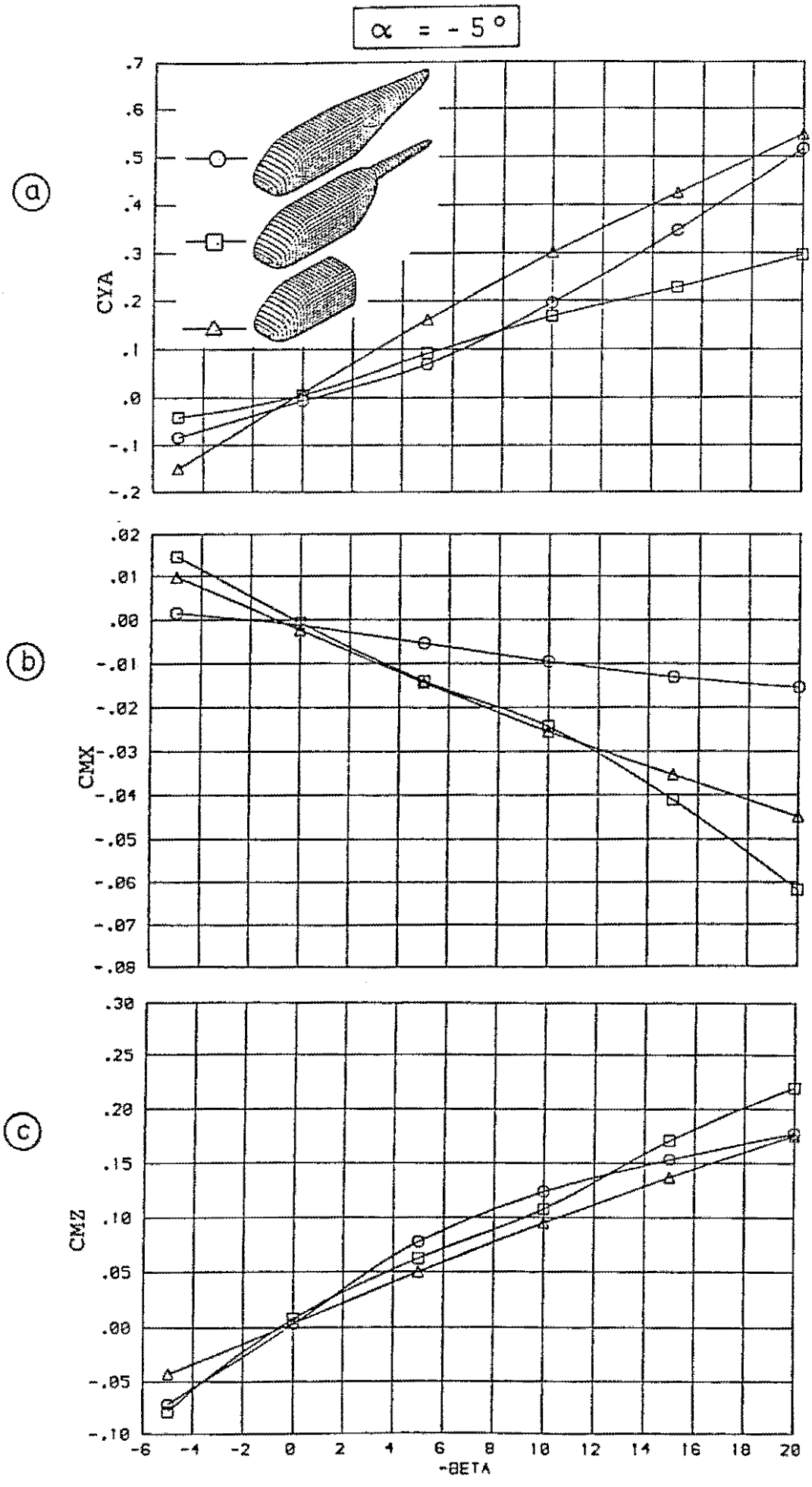

Fig. 6: Variation of Sideforce-, Rolling- and Yawing-moment coefficients with angle of yaw

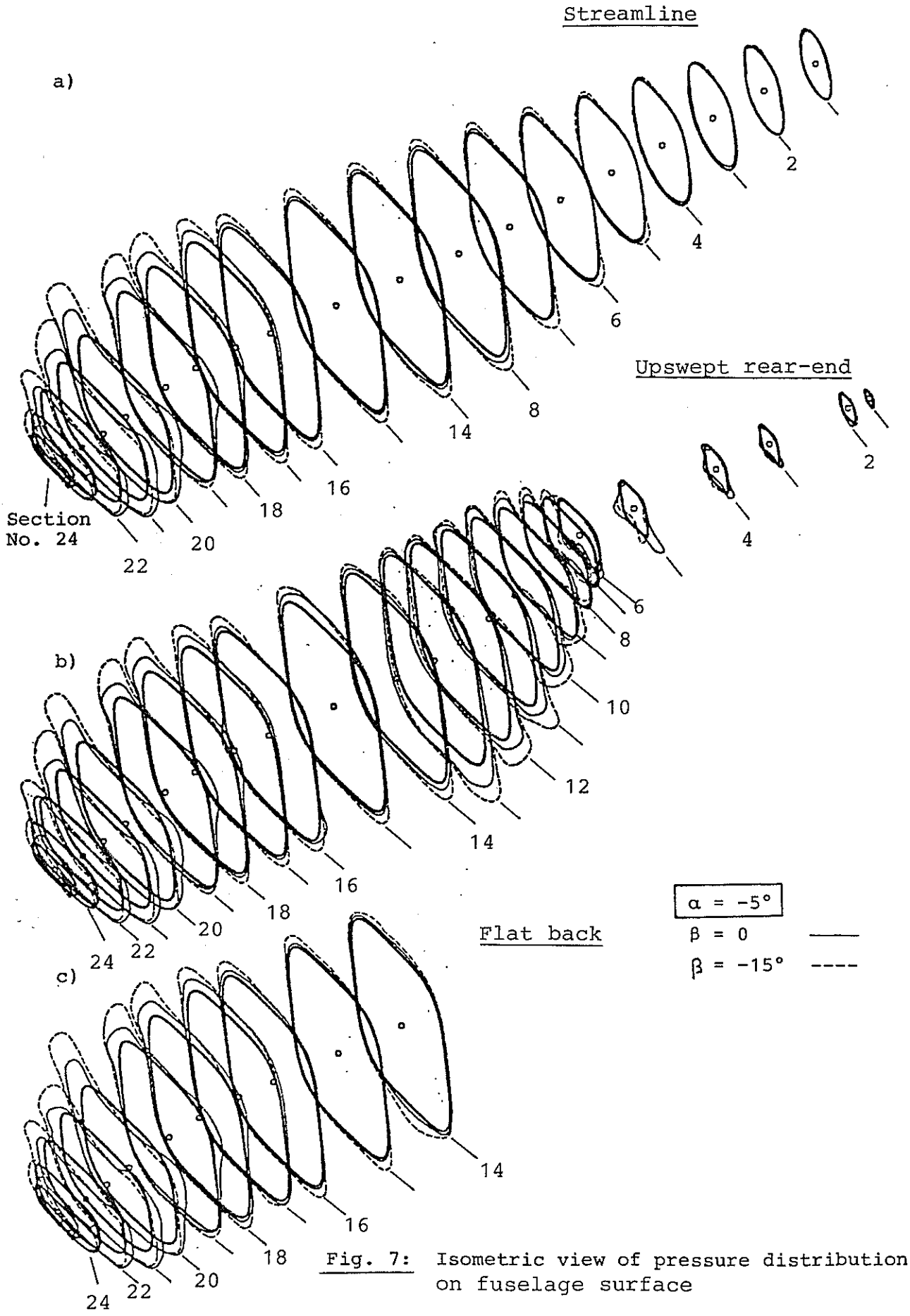

Fig. 7: Isometric view of pressure distribution on fuselage surface

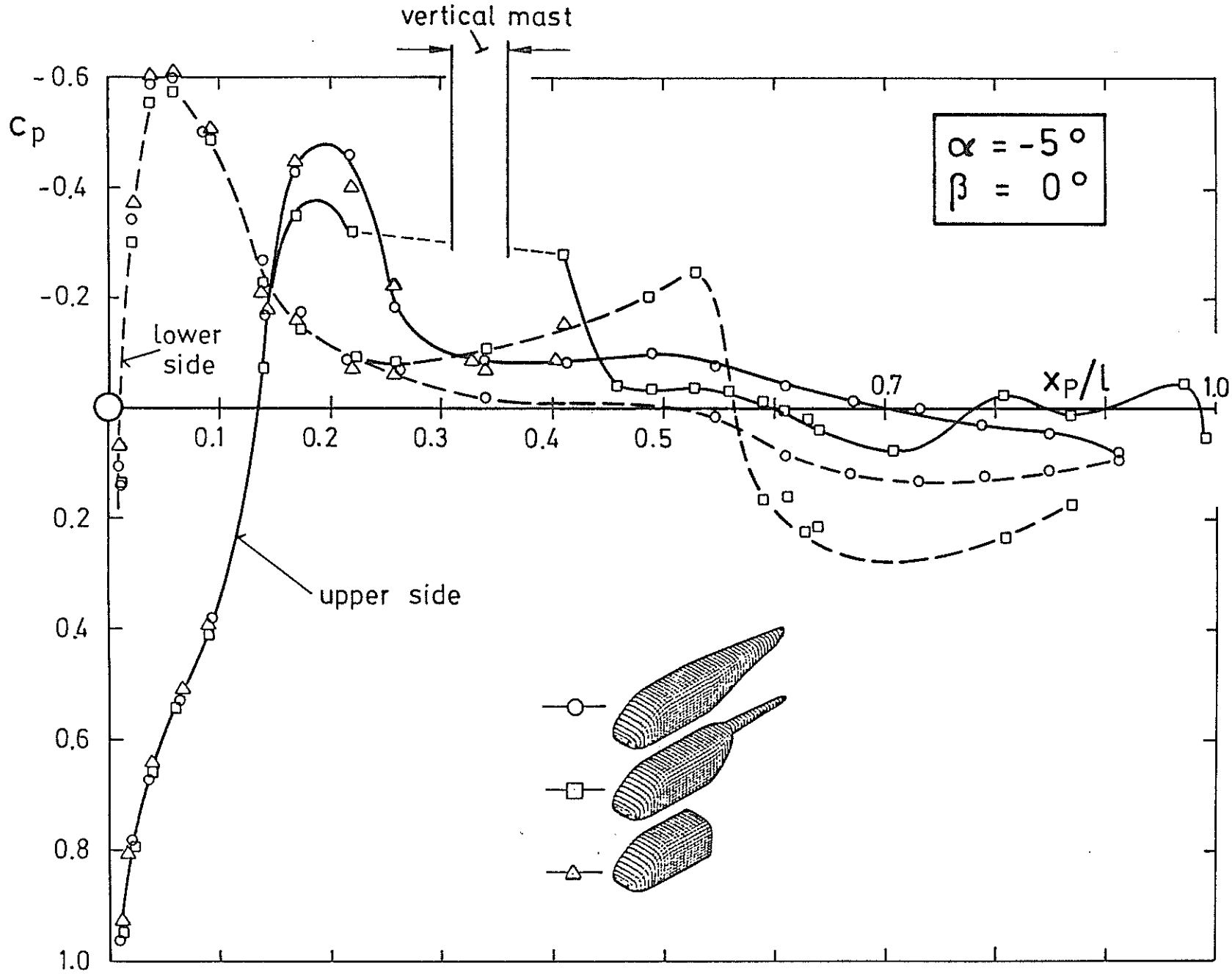

Fig. 8: Pressure distribution on upper and lower fuselage centre line

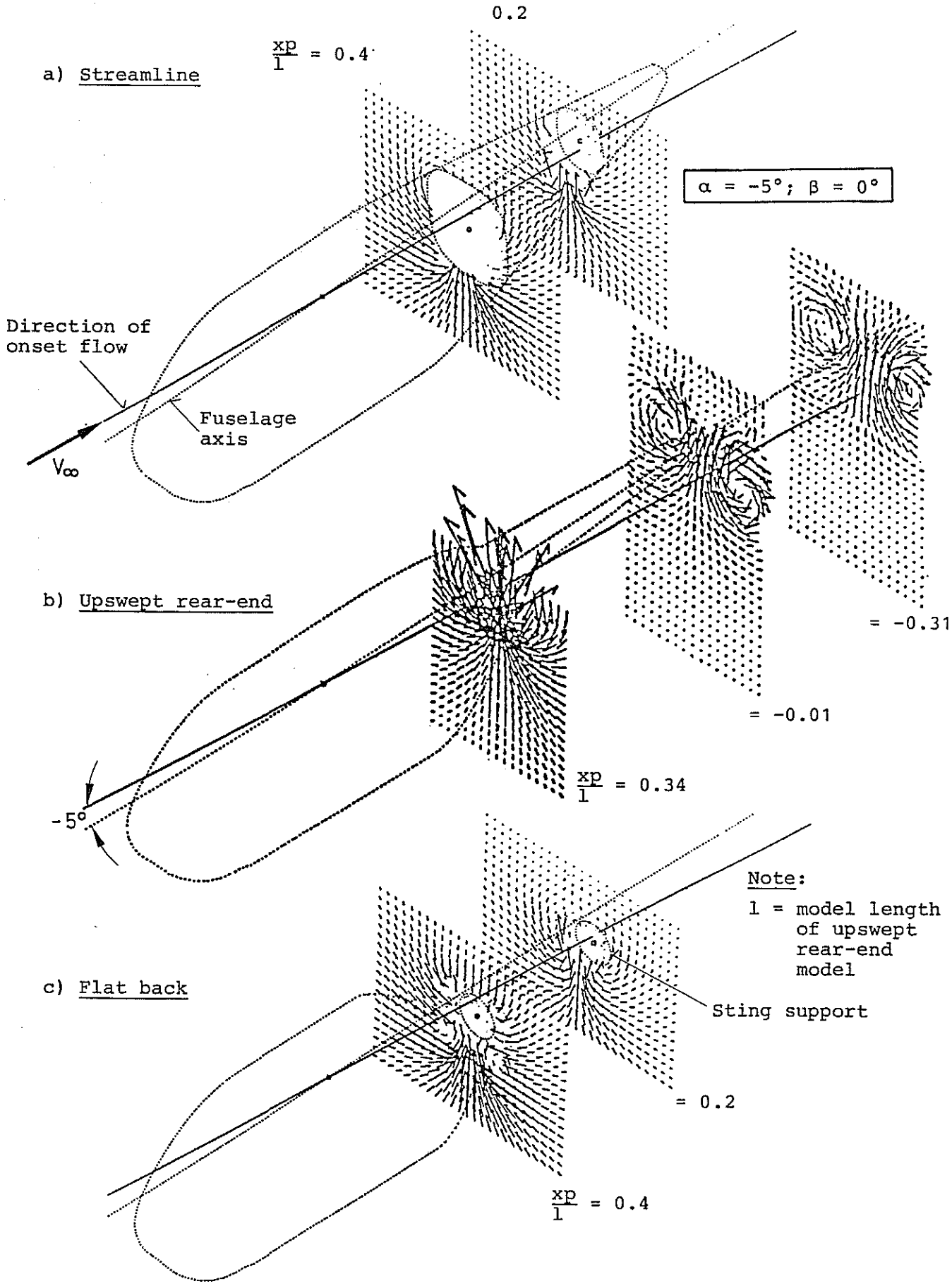

Fig. 9: Isometric view of cross flow velocity distribution in fuselage wake (V_{yz} vector plots)

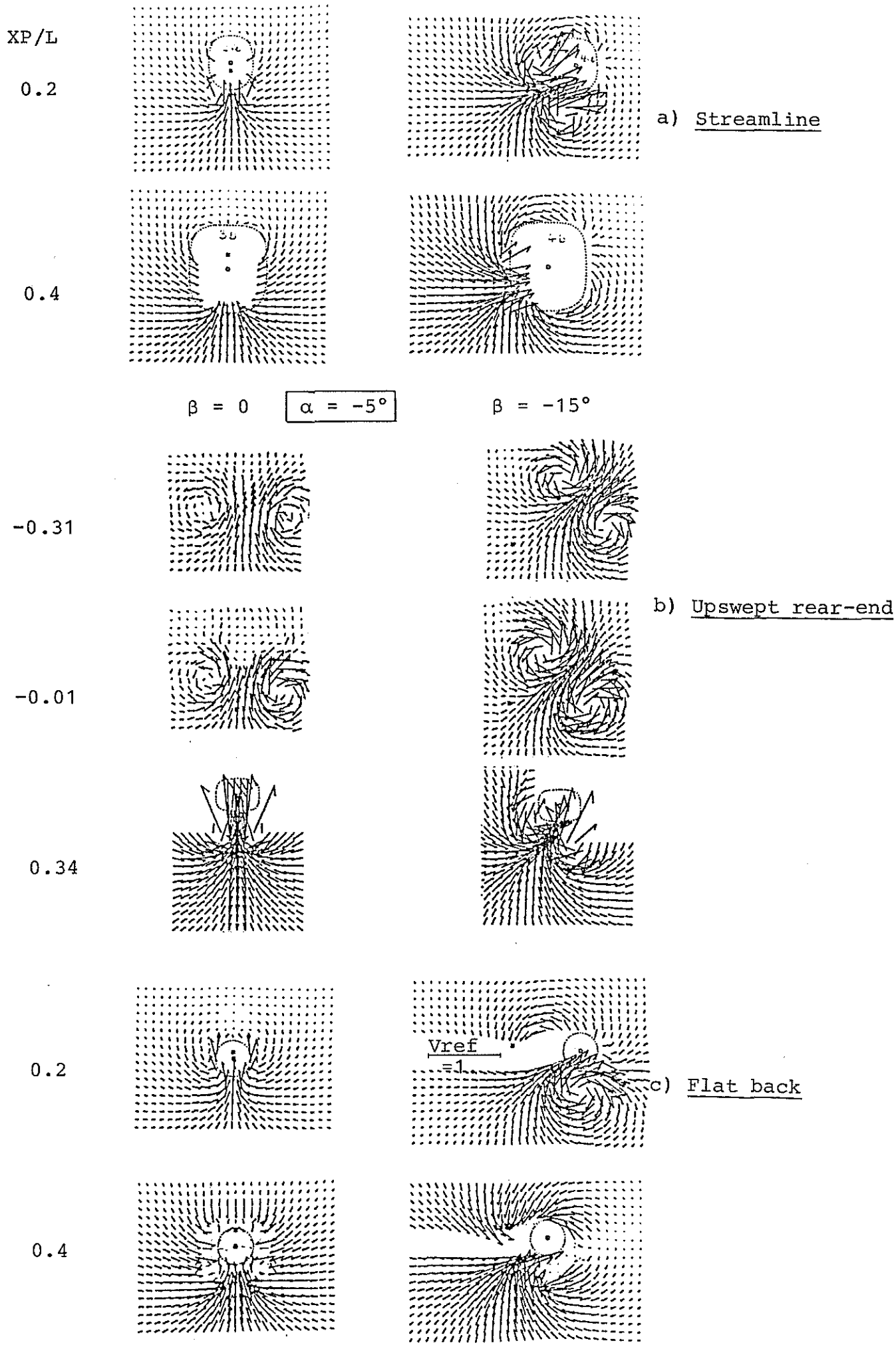

Fig. 10: Effect of yaw on cross flow velocity distribution in fuselage wake. Front view looking downstream.